World Academy of Science, Engineering and Technology
International Journal of Energy and Power Engineering
Vol:18, No:2, 2024

An Investigation on Designing and Enhancing the Performance of H-Darrieus Wind Turbine of 10 kW at the Medium Range of Wind Speed in Vietnam

Ich Long Ngo, Dinh Tai Dang, Ngoc Tu Nguyen, Minh Duc Nguyen

Open Science Index, Energy and Power Engineering Vol:18, No:2, 2024 publications.waset.org/10013504.pdf

Abstract**—**This paper describes an investigation on designing and enhancing the performance of H-Darrieus Wind Turbine (HDWT) of 10 kW at the medium wind speed. The aerodynamic characteristics of this turbine were investigated by both theoretical and numerical approaches. The optimal design procedure was first proposed to enhance the power coefficient under various effects, such as airfoil type, number of blades, solidity, aspect ratio, and tip speed ratio. As a result, the overall design of the 10 kW HDWT was well achieved, and the power characteristic of this turbine was found by numerical approach. Additionally, the maximum power coefficient predicted is up to 0.41 at the tip speed ratio of 3.7 and wind speed of 8 m/s. Particularly, a generalized correlation of power coefficient with tip speed ratio and wind speed is first proposed. These results obtained are very useful for enhancing the performance of the HDWTs placed in a country with high wind power potential like Vietnam.

Keywords**—**Computational Fluid Dynamics, double multiple stream tube, H-Darrieus wind turbine, renewable energy.

I. Introduction

NOWADAYS, an energy demand has played a very important role in producing and recovering the economy and society of any country. According to a report of International Renewable Energy Agency (IRENA), the global investment in energy transition technologies, including energy efficiency, reached a record high of USD 1.3 trillion in 2022 [1]. Among the variety of energy resources, renewable energy is still a top priority for energy security with the highest annual global investment recorded from 2015 to 2022 [1]. In recent years, wind power is being considered as one of the most potentially renewable energy resources because it has numerous advantages, including a small impact on the environment. Indeed, wind power capacity of the world increased from 23.9 GW (2001) to 539.581 GW (2017) [2]. In Vietnam, the wind power resource was reported to have a very high potential. According to the Vietnam Energy Association, technical potential for onshore wind is around 217 GW and total wind power capacity of 6 GW is targeted in the current national electricity development plan [3]. Additionally, based on the data of world bank, up to 39 percentages of the territory area were estimated to have wind speed higher than 6 m/s at an altitude of 65 m [4]. Therefore, many wind farms have been built in recent years, particularly in some provinces such as Soc Trang, Bac Lieu, Ninh Thuan, Binh Thuan, Ca Mau, and the Central Highlands [3], [5].

One of the most potential wind turbines is HDWT, which was invented first patented in 1931 by Darrieus, a French aviation engineer [6]. This type of vertical axis wind turbine (VAWT) has many advantages compared to horizontal axis wind turbine (HAWT), such as omni-directional capacity, simple structure, low noise. In addition, HDWT allows the generator and gearbox possibly be placed on the ground to reduce installation and maintenance costs [4], [7]. However, until now, the power coefficient of a general HDWT is still shown to be relatively low and the problem of self-starting ability has not been solved [8]. This becomes a challenge in both designing and manufacturing a wind turbine with higher efficiency.

To design and enhance the performance of HDWT, some approaches with results obtained have been proposed. First, theoretical models have been developed for this wind turbine, such as vortex model, Cascade model, single stream tube model, double stream tube model, and double multiple stream tube (DMST) model [9], [10]. Among these models, the DMST model has been widely used because it has low computational cost, fast prediction, good agreement with experimental results [10]. Recently, Ghiasi et al. [11] also used this model to examine the performance of HDWT with various effects, such as solidity, number of blades, airfoil types. Therefore, DMST has high potential for effective prediction, parametric study on HDWTs [12], [13]. Second, experimental studies were also performed to examine various aspects of VAWT. For example, Du et al. [14] experimentally considered many effects such as pitch angle, surface roughness, particularly self-starting capability, on the performance of HDWT. Additionally, Molina et al. [15] examined the effects of turbulent conditions and concluded that the power coefficient increases up to 20% as a turbulent intensity increases from 0.5% to 15%. The effects of flow uniformity on vibration and power generation of a small VAWT were studied by Sarkar et al. [16]. Meanwhile, Su et al. [17] proposed a new VAWT with a fixed main blade combined with rotatable auxiliary blades, and reported that better self-starting performance and higher power coefficient were obtained compared to a traditional HDWT when the wind speeds varied from 4.54 m/s to 8.82 m/s.

In recent years, the computational fluid dynamic (CFD) approach has also been considered as a promising candidate for investigating the characteristics and operating performance of

Ich Long Ngo is with Hanoi University of Science and Technology, Vietnam (e-mail: long.ngoich@hust.edu.vn).

Open Science Index, Energy and Power Engineering Vol:18, No:2, 2024 publications.waset.org/10013504.pdf

the HDWT [18], [19]. For example, Elsakka et al. [20] used CFD to analyze the effects of the angle of attack on the power generation of VAWT. These authors continued this research trend to validate the results from CFD models compared with the experimental data [21]. Additionally, Rogowski et al. [19] numerically studied the performance of HDWT with many types of 4-digits NACA airfoil. More recently, many researchers focus on blade pitching technologies to solve the low power coefficient problem of VAWT [22]-[24]. Although the HDWT has been studied by aforementioned approaches with results obtained, no research simultaneously considers the optimal design for almost important parameters, i.e., airfoil type, number of blades, solidity, aspect ratio, and tip speed ratio. Particularly, no research proposes a generalized correlation of power coefficient with respect to tip speed ratio and wind speed.

The objective of this study is to optimize and design a 10 kW HDWT at the medium range of wind speed. First, almost important parameters of the HDWT are simultaneously optimized by theoretical approach with the code development of DMST model. Second, the overall design of this wind turbine was built elaborately. Third, the CFD method was used to effectively predict the performance and aerodynamic characteristics of the HDWT designed from the previous step. Finally, a generalized correlation was revealed using a fitting method.

II. Theoretical and Numerical Methodology

A. Theoretical Model

To optimize the power coefficient of HDWT, the DMST model was first developed and used during the optimal design process. This is because this model was well validated and widely used for VAWTs including HDWT. It was first proposed by Parachiuvoiu et al. [25]. A basic idea lies in representing the air flow through a VAWT as a pair of actuator disks in tandem. More details of this model can be referred to Parachiuvoiu's book [26]. In the present study, the DMST model was programed in MATLAB [27]. Input data such as aerodynamic characteristics (i.e., lift and drag coefficients) were summarized from various literature including Parachiuvoiu's data [29]. Notably, since the upwind and downwind functions form a complex integral, numerical divergence frequently occurs, thus no results can be found. This integral problem was solved by directly applying the SIMPSON's 1/3 rule [28] during the code implementation.

Fig. 1 shows the validation of the present DMST model compared with Parachiuvoiu's model [29]. In this figure, tip speed ratio is defined as $\lambda = \omega R/V_\infty$, where ω, R, and V_∞ denote for angular velocity, radius of turbine, and freestream wind velocity, respectively. This figure indicates that the present results are in a very good agreement with those obtained by Paraschivoiu et al. [29] for whole range of λ. The deviation for most points is less than 1% and maximum deviation is also less than 10% at $\lambda = 2.5$. A slight discrepancy available here is due to the computational errors.

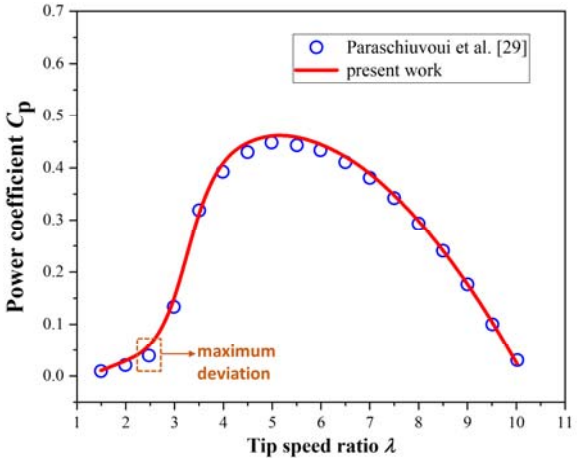

Fig. 1 Comparing results from the present DMST with those obtained by Paraschiuvoui et al. [29], for NACA0015 and $\sigma = 0.13$

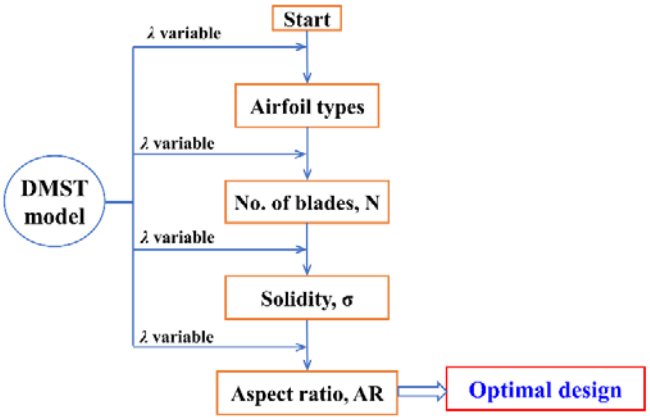

Fig. 2 The overall procedure for optimal design of a HDWT

Fig. 2 shows the designing procedure of a HDWT with the required power (P_r) and the range of V_∞. This procedure consists of the following steps: At start, power coefficient (C_p) and other input parameters, such as airfoil type, number of blades (N), solidity (σ), aspect ratio (AR), are initiated. Those parameters are sequentially entered into the DMST model programmed in MATLAB with λ varying in a specific range. As a result, the power and maximum power coefficient (C^*_{Pmax}) is determined temporally. New C_p is assigned for the next step. When the optimization is implemented for airfoil type, the remaining parameters are kept constant from the previous step. This process is repeated from airfoil type to aspect ratio, as illustrated in Fig. 2. All optimized parameters of the HDWT are delivered to optimal design step. Using this procedure, P_r can be obtained, and C_p reaches maximum value through all steps. Based on optimized parameters, other parts of HDWT, such as turbine shaft, strut, etc., are also calculated and designed accordingly. The technical drawings are consequently built. The results will be analyzed and discussed in Section III.

B. Numerical Model

In the first phase of our project, HDWT was designed for the required power of 10 kW using the optimum procedure mentioned in Section II *A*. To predict quickly and effectively

Open Science Index, Energy and Power Engineering Vol:18, No:2, 2024 publications.waset.org/10013504.pdf

the performance of the designed HDWT before manufacturing, the CFD method was applied. Additionally, this approach can also help to reduce the total costs of building a farm of HDWT. Moreover, 3D CFD simulation can be applied to capture the secondary flow and tip vortex effects that significantly impact the performance capability of a wind turbine in general.

The governing equations were used to describe the air flow through the HDWT, including continuity and Reynolds Averaged Navier-Stokes (RANS) equations. These equations were shown in (1) and (2), respectively, where ρ, μ, u, and p are air density, viscosity, local velocity, and local pressure, respectively. The last term on the right-hand side of (2) is known as the Reynold stress that leads to many turbulent models including k-ε and k-ω models. In the present study, k-ω Shear-Stress Transport (SST) model was applied. This is because this model has been highly recommended for simulating the turbulent flow through a wind turbine, as reported in literature [19], [30]. The governing equations of this model were shown in (3) and (4) for turbulent kinetic energy (k) and its dissipation rate (ω), respectively.

$$\frac{\partial \rho}{\partial t}+\frac{\partial}{\partial x_i}(\rho u_i)=0 \tag{1}$$

$$\frac{\partial}{\partial t}(\rho u_i)+\frac{\partial}{\partial x_j}(\rho u_i u_j)=-\frac{\partial p}{\partial x_i}+ \\ +\frac{\partial}{\partial x_j}\left[\mu\left(\frac{\partial u_i}{\partial x_j}+\frac{\partial u_j}{\partial x_i}-\frac{2}{3}\frac{\partial u_k}{\partial x_k}\delta_{ij}\right)\right]+\frac{\partial}{\partial x_j}\left(-\rho\overline{u_i' u_j'}\right) \tag{2}$$

$$\frac{\partial}{\partial t}(\rho k)+\frac{\partial}{\partial x_i}(\rho k u_i)=\frac{\partial}{\partial x_j}\left(\Gamma_k\frac{\partial k}{\partial x_j}\right)+G_k-Y_k+S_k \tag{3}$$

$$\frac{\partial}{\partial t}(\rho \omega)+\frac{\partial}{\partial x_i}(\rho \omega u_i)=\frac{\partial}{\partial x_j}\left(\Gamma_\omega\frac{\partial \omega}{\partial x_j}\right)+G_\omega-Y_\omega+D_\omega+S_\omega \tag{4}$$

The empirical constants of the k-ω SST model are:

$$\beta^*=0.09;\ \sigma_{k1}=0.85;\ \sigma_{k1}=1.0;\ \sigma_{\omega1}=0.5;\ \sigma_{\omega2}=0.856;$$
$$\gamma_1=0.5532;\ \gamma_2=0.4404;\ \beta_1=0.075;\ \beta_2=0.0828;\ \alpha_1=0.31$$

In (3) and (4), G_k is the generation of turbulence kinetic energy due to mean velocity gradient. G_ω is the generation of ω. Y_k and Y_ω are the dissipation of k and ω due to turbulence. D_ω is the cross-diffusion term. S_k and S_ω are user-defined source terms [31].

The geometrical model used in CFD simulation was shown in Fig. 3. In this model, the HDWT was run in a control volume with the dimensions of $20D\times10D\times5D$, where D is the turbine diameter. The turbine was placed at the distance of $5D$ from the inlet. Mesh motion was applied for modeling the rotation of turbine, thus two interface couples were required, as shown in Fig. 3. Additionally, the boundary conditions (BC) were also shown in this figure. A uniform velocity of relative wind was assumed to be used at the inlet while the zero pressure BC was specified at the outlet. The no-slip BC was used for surfaces of turbine blades. In addition, symmetry BC was used for the remaining surfaces of the computational domain.

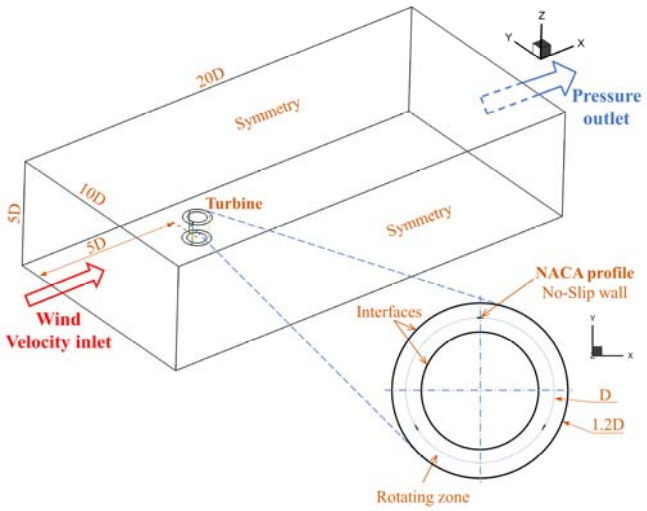

Fig. 3 Numerical model

The SIMPLE scheme was used for the pressure-velocity coupling with the potentiality in calculation time. Second-order upwind was specified for momentum, turbulent kinetic energy, and dissipation rate. In the numerical viewpoint, this scheme is to enhance the result accuracy. In addition, the time step size was set at 1 degree of azimuthal angle. The maximum iteration number per time step was specified at 40 in such a way that the numerical problem can be converged up to the residual of 3×10^{-4}. Finally, the computational data are recorded at the steady state to guarantee that the relative deviation of C_p between the preceding and backward revolutions is less than 2%.

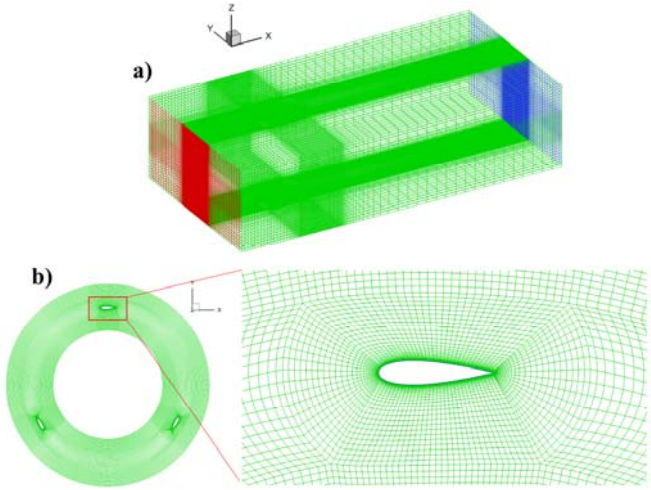

Fig. 4 Mesh model with structure mesh type: (a) Whole model and (b) Mesh layers surrounding turbine blade

The grid model was generated by Ansys ICEM-CFD with a structural mesh type used in all regions, as shown in Fig. 4 (a). In the direction normal to the airfoil surface, layers with the growth rate of 1.15 were controlled. As illustrated in Fig. 4 (b),

the thickness of the first layer near the airfoil wall is 3×10^{-4} m that corresponds to $y+ \approx 10$ for an initial estimation. Based on the simulation, the maximum value of a wall $y+$ obtained is less than 41 for all considered range of V_∞ and λ. The highest $y+$ distributed at the leading edge of turbine blade with the high wall shear stress. Mesh convergence test was conducted for five mesh models, from coarse to finer. The relative error decreases as the number of cells increases, as shown in Fig. 5. It means the mesh intends to converge. The selected point of the mesh model shown in Fig. 5 has a relative error of less than 3% compared with finest mesh model. As a result, this mesh model with 1,573,136 cells was used for all computations in this study.

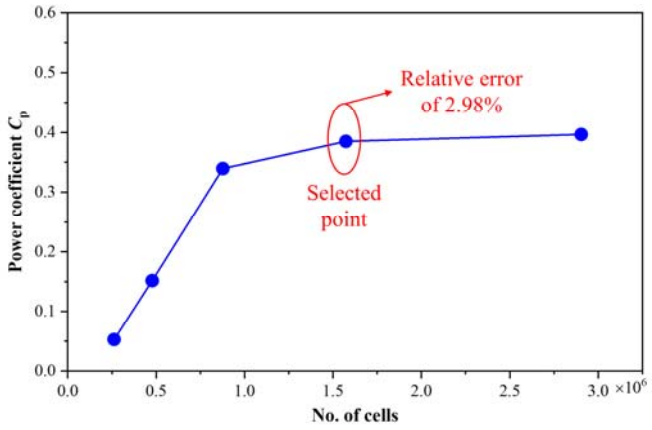

Fig. 5 Mesh convergence tests for NACA0015 and $\lambda = 2.52$

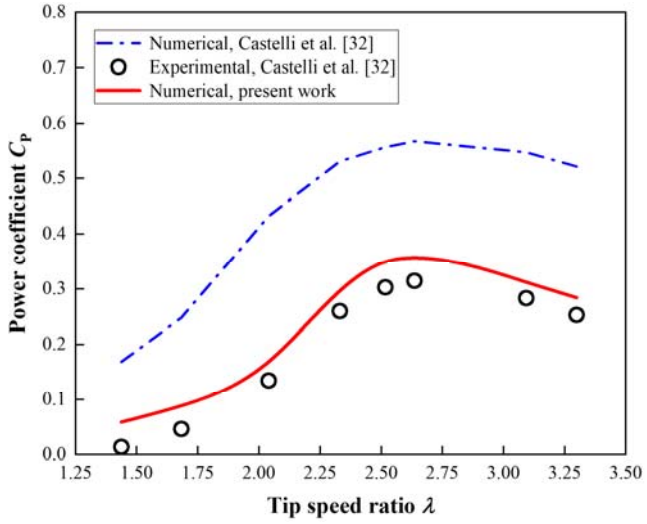

Fig. 6 Validation of numerical model compared with both numerical and experimental results from Castelli et al. [32]

The numerical model mentioned at the beginning of Section B was validated by comparing results from present work with both numerical and experimental results obtained by Castelli et al. [32]. λ varies from 1.4 to 3.3. The results are shown in Fig. 6. It was found that the variation of C_p with λ obtained for present work is in good agreement with that of Castelli's study. Furthermore, results from present study are closer to experimental results, even compared with the numerical results by the same author. Apart from first two points of small λ, the deviation between present results and experimental ones is less than 25%. Therefore, the numerical model was well validated, and it can be used for further computations in the present study.

III. Results and Discussions

A. Optimum Design

By using the designing procedure provided in Section II *A*, the important parameters of 10 kW HDWT are optimized. Airfoil types (NACA0012, NACA0015, NACA0018, NACA0021, and NACA0025) which significantly affect the aerodynamic characteristics of the HDWT are examined. The number of blades (i.e., 2, 3, 4, and 5 blades) was then considered. Solidity was defined as $\sigma = Nc/R$. In the present study, the solidities of 0.15, 0.2, 0.25, and 0.3 were tested. Additionally, aspect ratios $AR = D/H$ of 0.5, 1, and 1.5 were examined.

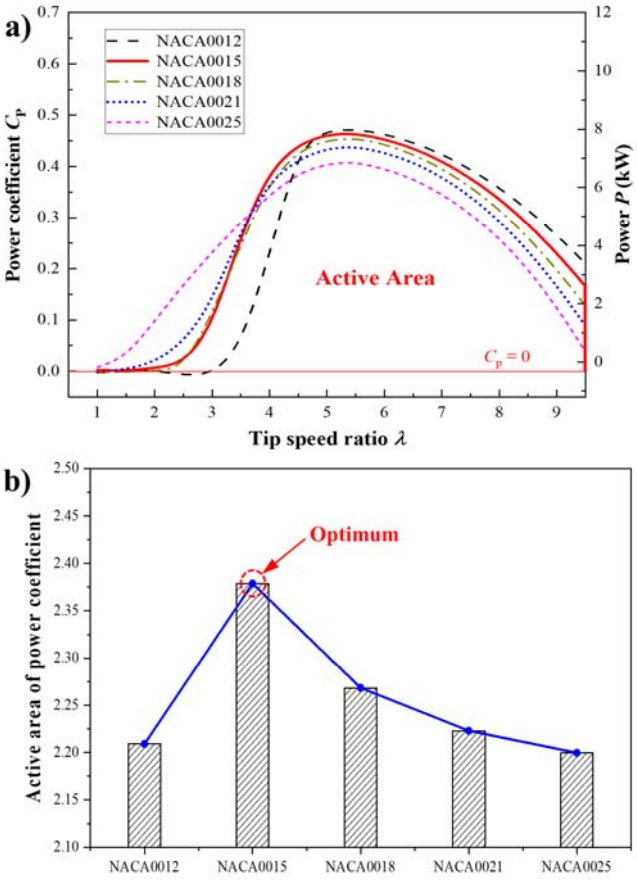

Fig. 7 (a) Power coefficient as a function of tip speed ratio for various types of NACA profile, and (b) determining optimal type of NACA profile

Fig. 7 shows in detail how to find the optimal type of NACA profile. The variation of power coefficient and even power with tip speed ratio are obtained for various types (Fig. 7 (a)). An active area confined by C_p-λ curve and a horizontal line $C_p = 0$, is calculated using an integral technique, and results are shown in Fig. 7 (b). Based on these results, an optimum design point

Open Science Index, Energy and Power Engineering Vol:18, No:2, 2024 publications.waset.org/10013504.pdf

of NACA profile is found quantitatively. The maximum value of the active area obtained is up to 2.38 for NACA0015, thus this profile type is applied for the next optimization process. It resembles other parameters mentioned previously. Consequently, the optimal parameters of the 10 kW HDWT were obtained, as provided in Table I.

TABLE I
DESIGNED PARAMETERS OF 10 KW HDWT

Airfoil	NACA0015
Number of blade (N)	3
Solidity (σ)	0.13
Chord length (c) [m]	0.22
Rotor radius (R) [m]	5
Rotor height (H) [m]	10

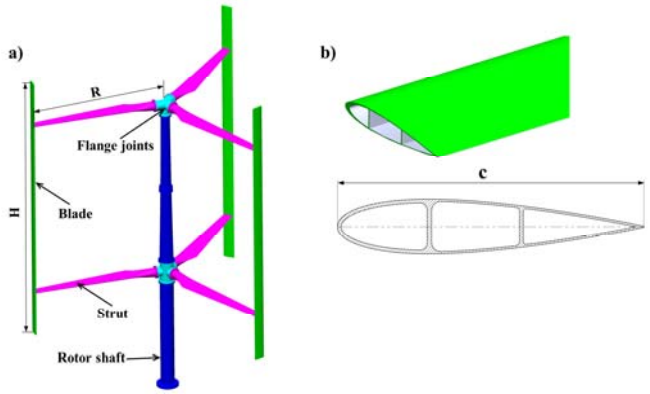

Fig. 8 The 10 kW HDWT: (a) overall design, (b) detailed structure of a NACA0015 blade

The overall design of 10 kW HDWT obtained was shown in Fig. 8 (a) based on parameters in Table I. Meanwhile, the detailed structure of a blade is illustrated in Fig. 8 (b). The blade has a hollow frame structure, and it was designed to achieve high durability and low blade weight. Furthermore, additional components of this turbine, such as strut, flange joint were designed based on the results obtained from previous studies [33], [34]. Notably, the specific strut was designed to ensure durability and improve the resonant frequency of this wind turbine.

B. Aerodynamic Characteristics

Fig. 9 shows the variation of power coefficient with respect to the azimuth per revolution for only blade #1 (Fig. 9 (a)) and for all three blades (Fig. 9 (b)). This result was computed based on the flow field from CFD method. Velocity contours of four particular positions of blade 1 were therefore shown in Fig. 10, that correspond to four points (#1, #2, #3, and #4) in Fig. 9 (a). At beginning, a negative C_P is available at the zero azimuth. This is because very low lift and drag resulted from symmetric airfoil at zero angle of attack (AoA), thus a slight difference in the velocity distribution between the upper and lower surface of blade #1, as shown in Fig. 10 (a). Then, C_P slightly decreases when the azimuth arises from 0° to around 20°, but this direction was changed for the azimuth ranging from 20° to around 90°. The maximum value of local C_P reaches the azimuth of about 90° that corresponds to point #2 in Figs. 9 (a) and 10 (b). This extreme point can be explained as follows: AoA is so high that the lift might reaches maximum (the significant difference in the velocity distribution between the upper and lower surface shown in Fig. 10 (b)) while the drag is still small; in addition, the turbulent wake is theoretically not available at the upstream part, thus C_P generated in this range of azimuth is highest accordingly.

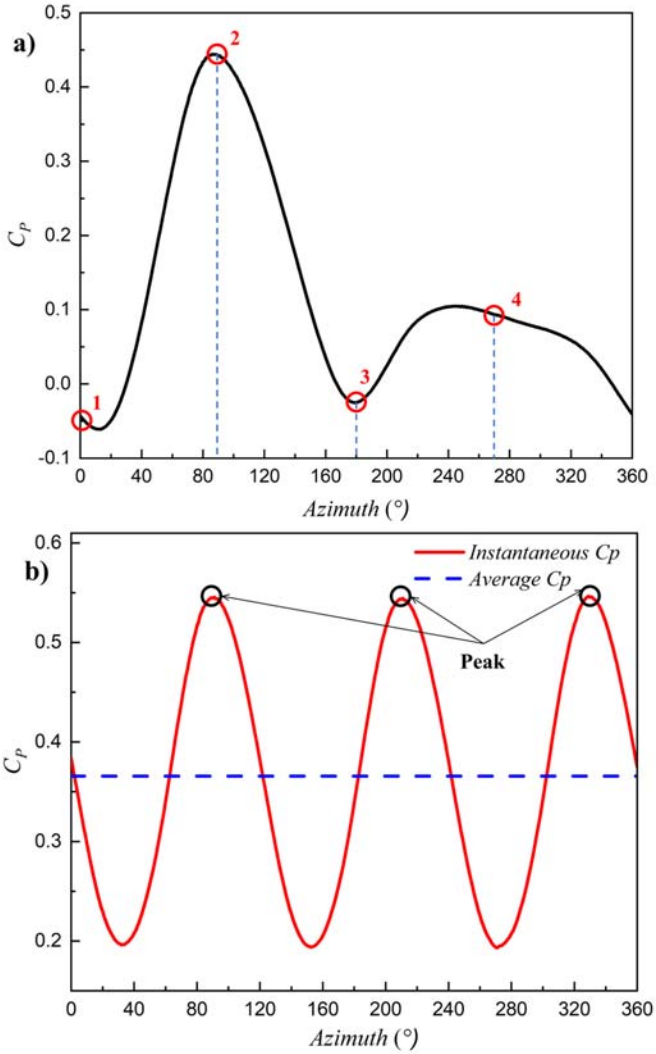

Fig. 9 Power coefficient as a function of azimuth at V_∞=7 m/s and λ = 3.8: (a) for blade #1, (b) for three blades

When the azimuth arises from 90° to around 180°, the C_P dramatically decreases, but it is in opposite direction compared with previous stage (20° to 90°). This is because the aerodynamic characteristic reduces when AoA becomes negative, as illustrated in Fig. 10 (c). The behaviors of the downstream part (the azimuth from 180° to 360°) are similar to the upstream part, however, the C_P generally lower due to the reduction of wind velocity and the appearance of turbulent wake. This result can be observed in Figs. 10 (d) and (e) for a detailed and general view, respectively. In this regard, the large region of very low velocity is distributed around the blade,

Open Science Index, Energy and Power Engineering Vol:18, No:2, 2024 publications.waset.org/10013504.pdf

resulting in the low lift and high drag, hence the C_P is obviously low. This is in line with the results reported in literature. These behaviors are similar for blade #2, and blade #3 with the phase difference of 120°.

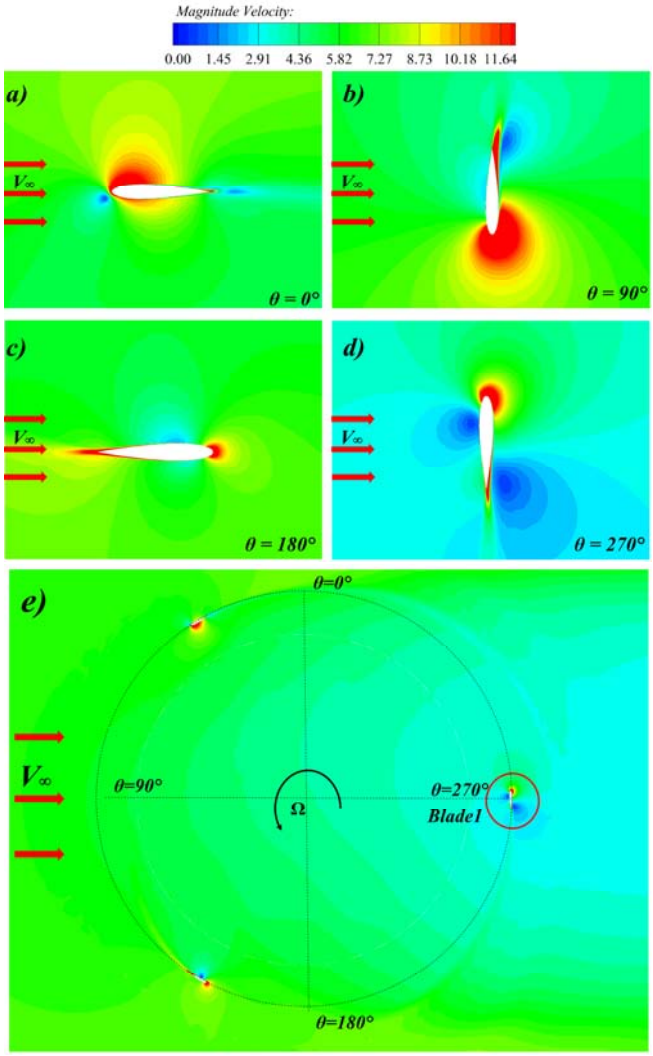

Fig. 10 Velocity contour on a middle plane (z = 0.0) for V_∞ = 7 m/s and λ = 3.8 around blade #1: (a) θ = 0°, (b) θ = 90°, (c) θ = 180°, (d) and (e) θ = 270°

Fig. 11 shows effects of wind speed on the turbulent flow characteristic around the HDWT designed. Therefore, the vorticity contour on the iso-surface of Q-criterion is obtained for wind speed value of 6 m/s (Fig. 11 (a)), 7 m/s (Fig. 11 (b)), and 8 m/s (Fig. 11 (c)). Notably, the Q-criterion was defined as 0.5*(W×W-S×S), where W and S are denoted for vorticity magnitude and strain rate, respectively. As a result, the positive and high value of this parameter is to indicate the regions with high and dominated vorticity (red) compared to the viscous stress component (strain rate). It was found from Fig. 11 that both vortex layers and wake vortex are frequently formed for the whole considered range of wind speed. The number of vortex layers increases with increasing the wind speed, and the region of the wake vortex becomes larger accordingly, as evident from Figs. 11 (a)-(c). This is due to the essential phenomenon of wind flow moving through the rotating VAWT. However, this phenomenon may lead to difficulties in improving the wind turbine power.

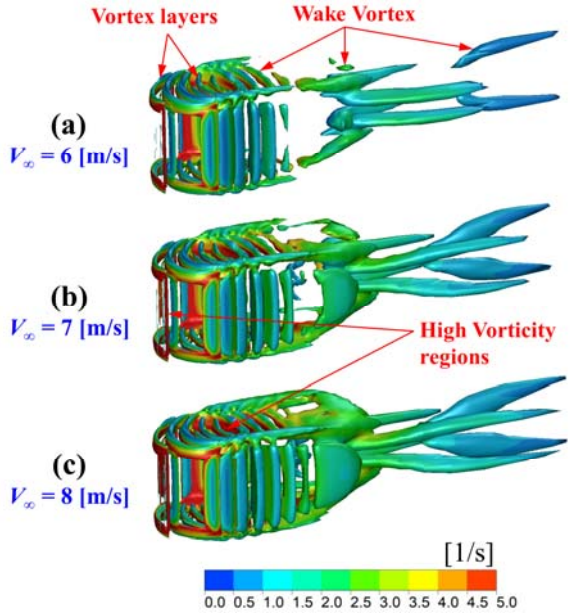

Fig. 11 Vorticity contour on an iso-surface of Q-Criterion for various wind speeds at λ = 5

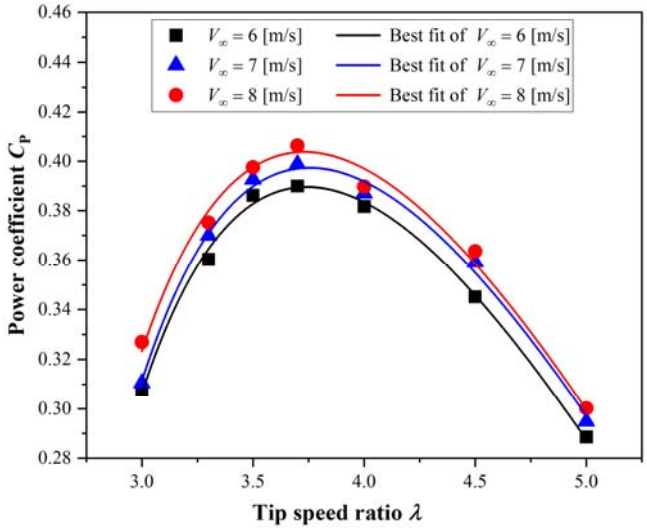

Fig. 12 The mean C_P as a function of TSR

The total C_P of HDWT for all three blades was also calculated, as shown in Fig. 9 (b). It was found that the variation of total C_P obeys sinusoidal law. Three peak points of C_P were obtained for three blades when they alternately passed through the position of θ = 90°. Notably, the mean C_P was also computed for each λ, as indicated by blue dash line in Fig. 9 (b). This was applied for various values of λ and V_∞ ranging from 6 m/s to 8 m/s. The results were therefore shown in Fig. 12. It was found from this figure that the maximum C_P obtained is up to around 0.41 at λ = 3.7 and wind velocity of 8 m/s. In addition,

Open Science Index, Energy and Power Engineering Vol:18, No:2, 2024 publications.waset.org/10013504.pdf

C_P increases with increasing V_∞, and it increases about 8.6% at the design point when V_∞ increases from 6 m/s to 8 m/s. This is a good guideline for enhancing the total efficiency of a general HDWT.

By fitting all data points shown in Fig. 12, a generalized correlation of power coefficient with both tip speed ratio and wind speed can be explored. This correlation is shown in (5). In the physical viewpoint, it is obviously seen that C_p reaches zero only if V_∞ or λ becomes zero. It implies that no power is created if no wind is available, or the turbine does not rotate due to a certain reason. Additionally, it was also found from (5) that C_p increases with increasing V_∞, whereas this trend is not unidirectional and depends on the value of λ. It means maximum power of a HDWT exists with respect to tip speed ratio. This was also reported in literature about wind turbines [26], [29]. Notably, (5) is valid for V_∞ ranging from 6 m/s to 8 m/s and λ ranging from 3 to 5. However, it can be developed and applied for the wider range of these parameters.

$$C_p = \frac{0.672 V_\infty^{0.136} \lambda^3}{0.02\lambda^6 + 60} \quad (5)$$

IV. Conclusions

The optimal study on designing the 10 kW HDWT at medium wind speed has been performed by both theoretical and numerical approaches. In the present study, the DMST model was programed in MATLAB, and the *k-ω* SST turbulence model was used to simulate the air flow through designed HDWT. The majority results are drawn as follows:

1) The designing procedure of a HDWT was first obtained in the present study in which the important parameters are optimized by theoretical DMST model.
2) The 10 kW HDWT operating at medium wind speed was well designed. This can be considered for turbine manufacturing or production in the future.
3) The characteristics and behaviors of designed HDWT were examined and analyzed using CFD method. The maximum C_P obtained is up to 0.41 at the tip speed ratio of 3.7 and wind velocity of 8 m/s.
4) A new correlation of power coefficient with tip speed ratio and wind speed was first proposed, as shown in (5).

Results obtained in the present study are very useful for enhancing the performance of a HDWT placed in a country with high wind power potential like Vietnam. They can be considered for the next phase in our project.

Acknowledgment

This research is funded by the Hanoi University of Science and Technology (HUST) under project number T2022-PC-017.

References

[1] IRENA and CPI 2020, "Global Landscape of Renewable Energy Finance," *International Renewable Energy Agency*, Abu Dhabi, pp. 10-29, 2023. ISBN: 978-92-9260-523-0

[2] L. Roy, K. Kincaid, R. Mahmud, and D. W. MacPhee, "Double-Multiple Streamtube Analysis of a Flexible Vertical Axis Wind Turbine," *Fluids*, vol. 6, no. 3, pp. 1-26, 2021.

[3] C.-N. Wang and T.-T. Dang, "Location optimization of wind plants using DEA and fuzzy multi-criteria decision making: A case study in Vietnam". *IEEE Access*, vol. 9, pp. 116265-116285, 2021.

[4] C. C. Nguyen, H. H. Le, and V. T. Nguyen, "Optimal aerodynamic design and generator matching for VAWT of 1kW using DMST method," *J. Tran. Scie. Tech*, vol. 7-8, pp. 179-184, 2013.

[5] N. Van Phong, N. T. Duong, and B. T. Son, "Liquefaction Characteristics of Sandy Soil Distributed in Wind Power Farms, Soc Trang Province, Vietnam," *The Iraqi Geological Journal*, vol. 55, no. 2E, pp. 219-229, 2022.

[6] P. M. Kumar, K. Sivalingam, S. Narasimalu, T. C. Lim, S. Ramakrishna, and H. Wei, "A Review on the Evolution of Darrieus Vertical Axis Wind Turbine: Small Wind Turbines," *Journal of Power and Energy Engineering*, vol. 7, no. 4, pp. 27-44, 2019.

[7] G. W. Song Chenguang, Zhu Weinan, Zhang Xudong, "Study on Aerodynamic Characteristics of Darrieus Vertical Axis Wind Turbines with Different Airfoil Maximum Thicknesses Through Computational Fluid Dynamics," *Arabian Journal for Science and Engineering*, vol. 45, no. 2, pp. 689-698, 2020.

[8] M. A. Dabachi, A. Rahmouni, E. Rusu, and O. Bouksour, "Aerodynamic Simulations for Floating Darrieus-Type Wind Turbines with Three-Stage Rotors," *Inventions*, vol. 5, no. 2, pp. 1-18, 2020.

[9] M. Islam, D. S. K. Ting, and A. Fartaj, "Aerodynamic models for Darrieus-type straight-bladed vertical axis wind turbines," *Renewable and Sustainable Energy Reviews*, vol. 12, no. 4, pp. 1087-1109, 2008.

[10] N. Batista, R. Melício, V. Mendes, M. Calderón, and A. Ramiro, "On a self-start Darrieus wind turbine: Blade design and field tests," *Renewable and Sustainable Energy Reviews*, vol. 52, pp. 508-522, 2015.

[11] P. Ghiasi, G. Najafi, B. Ghobadian, A. Jafari, and M. Mazlan, "Analytical Study of the Impact of Solidity, Chord Length, Number of Blades, Aspect Ratio and Airfoil Type on H-Rotor Darrieus Wind Turbine Performance at Low Reynolds Number," *Sustainability*, vol. 14, no. 5, pp. 2623, 2022.

[12] Z. Zhao, S. Qian, W. Shen, T. Wang, B. Xu, Y. Zheng, et al., "Study on variable pitch strategy in H-type wind turbine considering effect of small angle of attack," *Journal of Renewable and Sustainable Energy*, vol. 9, no. 5, pp. 1-21,2017.

[13] H. M. Mahdi Moghimi, "Developed DMST model for performance analysis and parametric evaluation of Gorlov vertical axis wind turbines," *Sustainable Energy Technologies and Assessments*, vol. 37, pp. 100616, 2020.

[14] L. Du, G. Ingram, and R. G. Dominy, "Experimental study of the effects of turbine solidity, blade profile, pitch angle, surface roughness, and aspect ratio on the H-Darrieus wind turbine self-starting and overall performance," *Energy Science & Engineering*, vol. 7, no. 6, pp. 2421-2436, 2019.

[15] C. Molina, T. De Troyer, T. Massai, A. Vergaerde, M. C. Runacres, and G. Bartoli, "Effect of turbulence on the performance of VAWTs: An experimental study in two different wind tunnels," *Journal of Wind Engineering and Industrial Aerodynamics*, vol. 193, pp. 103969 (1-20), 2019.

[16] M. R. Sarkar, S. Julai, M. J. Nahar, M. Uddin, M. Rahman, and M. R. Tanshen, "Experimental study of vertical axis wind turbine performance under vibration," *International Journal of Robotics and Control Systems*, vol. 1, no. 2, pp. 177-185, 2021.

[17] H. Su, B. Dou, T. Qu, P. Zeng, and L. Lei, "Experimental investigation of a novel vertical axis wind turbine with pitching and self-starting function," *Energy Conversion and Management*, vol. 217, pp. 113012, 2020.

[18] R. Firdaus, T. Kiwata, and T. Kono, "Numerical and experimental studies of a small vertical-axis wind turbine with variable-pitch straight blades," *Journal of Fluid Science and Technology*, vol. 10, no. 1, pp.x, 2015.

[19] G. B. Krzysztof Rogowski, Martin Otto Lacer Hansen, "Performance Analysis of a H-Darrieus Wind Turbine for a Series of 4-Digit NACA Airfoils," *Energies*, vol. 13, no. 12, pp. 3196, 2020.

[20] M. M. Elsakka, D. B. Ingham, L. Ma, and M. Pourkashanian, "CFD analysis of the angle of attack for a vertical axis wind turbine blade," *Energy Conversion and Management*, vol. 182, pp. 154-165, 2019.

[21] M. M. Elsakka, D. B. Ingham, L. Ma, and M. Pourkashanian, "Comparison of the computational fluid dynamics predictions of vertical axis wind turbine performance against detailed pressure measurements," *International Journal of Renewable Energy Research*, vol. 11(1), pp. 276-293, 2021.

[22] H. Huang, Z. Nong, G. Li, and J. Li, "Research and optimization of a built-in entity vertical axis wind turbine by variable pitch strategy," *Journal of Building Engineering*, vol. 68, pp. 105810, 2022.

[23] R. Shah, M. A. Jamal, T. I. Khan, and U. W. Qazi, "Experimental and

Open Science Index, Energy and Power Engineering Vol:18, No:2, 2024 publications.waset.org/10013504.pdf

Numerical Evaluation of Performance of a Variable Pitch Vertical-Axis Wind Turbine," *Journal of Energy Resources Technology*, vol. 144, no. 6, pp. 061303 (1-9), 2022.

[24] X. Sun, T. Hao, J. Zhang, L. Dong, and J. Zhu, "The performance increase of the wind-induced rotation VAWT by application of the passive variable pitching blade," *International Journal of Low-Carbon Technologies*, vol. 17, pp. 061303(1-9), 2022.

[25] Paraschivoiu and F. Delclaux,"Double multiple streamtube model with recent improvements (for predicting aerodynamic loads and performance of Darrieus vertical axis wind turbines)," *Journal of Energy*, vol. 7, no. 3, pp. 250-255, 1983.

[26] Paraschivoiu, "Wind Turbine Design: With Emphasis on Darrieus Concept," *Presses inter Polytechnique*. 2002.

[27] MATLAB, version R2016a, Natick, "Massachusetts," *The MathWorks Inc.*, 2010.

[28] S. C. Chapra and R. P. Canale, "Numerical methods for engineers," *McGraw-Hill New York*, vol. 1221, 2011.

[29] Paraschivoiu, O. Trifu, and F. Saeed,"H-Darrieus Wind Turbine with Blade Pitch Control," *International Journal of Rotating Machinery*, vol. 2009, pp. 1-7, 2009.

[30] M. Ning, H. Lei, Z. Han, D. Zhou, Y. Bao, K. Zhang, et al., "Airfoil optimization to improve power performance of a high-solidity vertical axis wind turbine at a moderate tip speed ratio," *Energy*, vol. 150, pp. 236-252, 2018.

[31] Fluent, A. N. S. Y. S. "ANSYS fluent theory guide, Release 19.1," *ANSYS inc.*, PA 33, pp. 373-464, 2013.

[32] E. Marco Raciti Castelli, Ernesto Benini, "The Darrieus wind turbine: Proposal for a new performance prediction model based on CFD," *Energy*, vol. 36, no. 8, pp. 4919-4934, 2011.

[33] Hand and A. Cashman, "Conceptual design of a large-scale floating offshore vertical axis wind turbine," *Energy Procedia*, vol. 142, pp. 83-88, 2017.

[34] H. Yichen Jiang, Peidong Zhao, Tiezhi Sun, "Investigation of Blade Tip Shape for Improving VAWT Performance," *Journal of Marine Science and Engineering*, vol. 8, no. 3, pp. 225, 2020.

Open Science Index, Energy and Power Engineering Vol:18, No:2, 2024 publications.waset.org/10013504.pdf